

N84 10154

A REVIEW OF NONEQUILIBRIUM EFFECTS AND SURFACE CATALYSIS  
ON SHUTTLE HEATING

Carl D. Scott  
NASA Johnson Space Center  
Houston, Texas

SUMMARY

This paper is a review of the nonequilibrium calculation techniques developed by various authors over the past decade to predict heat fluxes to the windward side of the Space Shuttle orbiter. The results of these techniques are compared with measurements made on the first few flights of the Space Shuttle. The calculations attempt to account for finite rate chemistry in the shock layer around the vehicle and for finite rate catalytic atom recombination on the thermal protection materials. The techniques considered are the axisymmetric viscous shock layer method, three-dimensional (3-D) reacting Euler equation solutions coupled with axisymmetric analog boundary layer method, and a recently developed nonequilibrium 3-D viscous shock layer method.

The comparisons indicate a substantial influence of nonequilibrium chemistry on the heating to the relatively noncatalytic thermal protection tiles of the orbiter. That is, the heat flux is much lower than if the flow were in equilibrium or the tiles were fully catalytic. It is shown that all of the methods agree with the measurements within about 10 to 30%, depending on the location, flight condition, and assumption about the catalytic recombination coefficients. None of the calculations could predict the measurements uniformly over the entire windward centerline for all flight conditions. (Until now the 3-D viscous shock layer calculations have only treated the noncatalytic wall.)

It is noted that for a given flight condition the temperature measured on the orbiter tended to increase from the second flight to the fifth flight. The cause of this increase is not known, but it may be due to contamination of the surface, causing an increase in catalyticity, or to a decrease in emittance.

Nitrogen recombination was found to be significant early in the entry especially in areas dominated by normal shock flow such as near the nose. This makes knowing the nitrogen recombination phenomena important. Such phenomena will be of more importance on an aerobraking orbital transfer vehicle which enters the atmosphere at higher velocities.

It is concluded that the nonequilibrium methodologies have significantly enhanced the capability to predict the heat flux for high altitude reentry, but some improvements are still required to improve the current accuracy.

## SYMBOLS

ALT altitude  
C atom mass fraction  
f heat flux adjustment factors defined in eq. (2)  
 $h_T$  total enthalpy  
k Boltzmann constant  
 $k_w$  catalytic recombination speed  
L length of vehicle  
 $\tau$  mass of atom  
P pressure  
q heat flux  
T temperature  
V velocity  
VIN $\infty$  freestream velocity  
X axial distance from nose  
Z geometric altitude

### Greek Symbols

$\epsilon$  emittance  
 $\gamma$  energy transfer catalytic combination coefficient

### Subscripts

FC fully catalytic  
N nitrogen  
O oxygen  
w wall  
 $\infty$  freestream  
ref reference condition or property

## INTRODUCTION

The Space Shuttle orbiter is a hypersonic glide reentry vehicle that spends much of its entry time at relatively tenuous altitudes in which chemical nonequilibrium predominates in the shock layer. Calculations have shown that both dissociation nonequilibrium<sup>1,2</sup> and recombination nonequilibrium exist<sup>1</sup>. The dissociated nonequilibrium exists in the inviscid layer and the recombination nonequilibrium exists in the boundary layer. Verification of these phenomena has not been directly obtained; however, these phenomena are inferred by comparing heat transfer measurements with the reacting flowfield results.

Although measurements of surface temperatures on the high temperature reusable surface insulation (HRSI) tiles have been made at numerous locations on the orbiter, this paper only addresses measurements on or near the windward centerline of the lower fuselage because predictions of local flow conditions are much easier to obtain in this region. The presence of chemical nonequilibrium was made easier to verify because the HRSI tile glass coating (RCG) is relatively noncatalytic with

respect to atom recombination and the associated dissociation energy accommodation. Also of great importance in demonstrating the nonequilibrium flow behavior is the catalytic surface effects orbiter flight experiment of Stewart, Rakich, and Lanfranco<sup>3</sup>, whose initial results were reported in reference 4. Prior to the flight experiments, predictions of the noncatalytic nature were reported in references 1, 2, and 3 based on flowfield computations and arc jet experiments. Besides the results reported in reference 4 other calculations have been made for the RCG coated tiles and compared with flight measurements. Scott and Derry<sup>5</sup> used the reacting flowfield/boundary layer method of reference 2 with measured energy transfer catalytic recombination coefficients of reference 6 and compared those predictions with flight measurements. Likewise, Shinn, Moss, and Simmonds<sup>7</sup> computed heat fluxes using an axisymmetric reacting viscous shock layer code with the recombination coefficients of reference 6 and showed better agreement with flight measurements. Recently Kim, Swaminathan and Lewis<sup>8</sup> solved the 3-D viscous shock layer equations for the Shuttle geometry, and obtained encouraging results.

This paper critically evaluates the various flowfield predictions, comparing the results of equilibrium and nonequilibrium flowfields coupled with reacting axisymmetric analog boundary layer solutions and the results of viscous shock layer solutions with flight temperature/heat flux measurements near the windward centerline for the Shuttle flights STS-2, 3, and 5.

In the comparisons with flight heat flux measurements there is concern with two basic aspects of the predictions, the flowfield methodology and the surface catalytic recombination phenomena. The first aspect can be subdivided into dynamical and geometrical characteristics, and thermophysical properties and gas phase chemical reaction kinetics. The second aspect can be subdivided into wall recombination rates of the basic thermal protection material, contamination issues, and knowledge gained from the catalytic surface effects experiment. All of these aspects are interrelated and the Shuttle flight does not provide an experiment in which each aspect can be controlled independently. Numerical simulation is capable of single parameter variation, but confirmation of the results is difficult because of flight complexities and unknowns; particularly, there is no measurement of the chemical composition of the flow. This paper considers flowfield chemical composition effects (equilibrium vs nonequilibrium), methods of solution (two-layer approaches and viscous shock layer approaches), and surface catalytic recombination rates, and it touches on possible contamination on the surface. The issues of incomplete chemical energy accommodation of catalytically-formed excited species and subsequent quenching are not explored.

#### COMPUTATIONAL METHODS AND THEIR APPLICATION

Five computational methods are considered here which are subdivided into applications of those methods, which are further subdivided into particular cases. These cases are summarized in Table 1.

The first two methods are axisymmetric viscous shock layer methods of Moss<sup>9</sup> and Miner and Lewis<sup>10</sup>. The next two are two-layer approaches. Rakich and Lanfranco<sup>2</sup> treated the 3-D reacting inviscid flowfield and used the results for reacting boundary layer edge conditions. Goodrich et al.<sup>11</sup> solved the equilibrium

3-D inviscid case and used their results as edge conditions for equilibrium boundary layer solutions. The fifth method is the 3-D nonequilibrium viscous shock layer method of Kim, Swaminathan and Lewis<sup>8</sup>.

Shinn, Moss and Simmonds<sup>7</sup> applied the Moss<sup>9</sup> method with variable wall recombination coefficients to the Shuttle orbiter by approximating the Shuttle geometry with hyperboloids of revolution fitted by Zoby<sup>12</sup>. They presented cases for various times in the orbiter entry and concluded the following. The Shuttle flight data indicates the shock layer flow is appreciably in nonequilibrium down to an altitude of 50 km. Scott's extrapolated recombination rates<sup>6</sup> used in their viscous shock layer calculations result in good agreement with flight data forward, but not aft, on the vehicle. Better agreement aft is obtained if  $k_{w0} = 100$  cm/sec is used. The temperature of the surface during entry is 80 to 200 K less than if it were fully catalytic.

Gupta, Moss, Simmonds and Shinn<sup>13</sup> similarly applied the Moss<sup>9</sup> method with various recombination coefficients and for a range of angle of attack of the orbiter. They found that a  $\pm 5^\circ$  variation in angle of attack does not affect the nonequilibrium heating appreciably at 75 and at 48 km altitudes. The temperature dependence of the oxygen recombination rate is not as steep as an extrapolation of Scott's<sup>6</sup> data indicates. They concluded that a value of  $k_{w0} = 200$  cm/sec seems to yield better agreement with the flight measurement of heat flux at certain locations and flight regimes. A 49% reduction in heating due to nonequilibrium effects was noted in the nose region at  $X/L = 0.025$  and 75 km altitude. Nonequilibrium effects on the heating are not significant below about 65 km even though the flow may not be in equilibrium, indicating that equilibrium boundary layer methods or heating correlations of the type suggested by Rakich et al.<sup>4</sup> may be useful.

The method of Rakich and Lanfranco<sup>2</sup> was applied by Rakich, Stewart and Lanfranco<sup>4</sup> to calibrate the results of an approximate method that uses equilibrium normal shock isentropic boundary layer edge conditions in lieu of the reacting variable entropy edge conditions. This approximate method was then used to infer  $k_{w0}$  of the reaction cured glass (RCG)-coated high temperature reusable surface insulation (HRSI) tiles and to infer  $k_{w0}$  of the iron-cobalt-chromia spinel (C742) coating used in the catalytic surface effects flight experiment tiles. They inferred that  $k_{w0} = 80$  cm/sec and assumed that  $k_{wN} = 0.3 k_{w0}$  for RCG at  $T_w$  of about 1100 K. Their catalytic surface effects experiment demonstrated that the flow is indeed in chemical nonequilibrium. Rakich's method was also used by Scott<sup>5</sup> with temperature dependent recombination coefficients inferred from arc jet measurements.<sup>6,14</sup> He used the reacting boundary layer code BLIMPK developed by Bartlett and Kendall<sup>15</sup> and extended by Tong, Buckingham and Morse<sup>15</sup>. This method resulted in higher heating than measured on the nose of the orbiter, but tended to predict or underpredict the heating on the midbody. These results are presented here for comparison with other results.

Reacting boundary layer calculations were made with equilibrium edge conditions provided by Goodrich et al.<sup>11</sup> along with different wall recombination assumptions. These results are presented here.

Miner and Lewis<sup>10</sup> axisymmetric, reacting viscous shock-layer code was applied with various catalytic wall assumptions and those results are likewise presented here.

The fifth computational method considered herein for nonequilibrium flow calculations applied to the Space Shuttle was presented by Kim, Swaminathan and Lewis<sup>8</sup>. That recent paper addressed the windward side of the Space Shuttle, applying the 3-D nonequilibrium shock layer method with noncatalytic boundary conditions. Their windward centerline results for two points in the STS-2 trajectory are presented here.

#### MEASUREMENTS OF HEAT FLUX TO SHUTTLE

Surface temperature measurements of several instrumented HRSI tiles, distributed along the lower surface of the orbiter, are considered in this paper. The flights considered are STS-2, 3, and to a limited extent STS-5. Trajectory information was obtained from acceleration measurements on the orbiter and from atmosphere models calibrated by atmospheric soundings. The resulting best estimated trajectories (BET) were obtained from the Johnson Space Center, Mission Planning and Analysis Division. Heat fluxes were inferred from the measured temperatures by computing the corrected radiation equilibrium heat flux

$$q = 1.06 \epsilon \sigma T_w^4 f \quad (1)$$

The factor 1.06 accounts for the fact that the thermocouples lie about 0.38 mm beneath the surface coating and for conduction in the tile. This factor was obtained from the method of Williams and Curry<sup>17</sup> who inferred heat fluxes from temperatures using an inverse thermal math model formulation\*. Over the range of time in the trajectory and temperatures considered in this paper, a correction factor of 1.06 is accurate to within 2 or 3 percent.

When comparing the measurements of one flight with another or when comparing calculations with measurements it is necessary to adjust the heat fluxes to account for differences in freestream conditions. Since the hypersonic stagnation point heating is approximately proportional to  $(\rho/\rho_{ref})^{1/2} (V/V_{ref})^3$  all points were corrected by the ratio of that factor for the two freestream conditions, i.e.,

$$f = (\rho_{\infty} / \rho_{\infty ref})^{1/2} (V_{\infty} / V_{\infty ref})^3 \quad (2)$$

The flight BET and the flight heating rates are used as reference conditions when flight measurements are compared with calculations. The heat fluxes are then presented in absolute units as obtained from equation (1). The factor  $f$  is probably accurate to within  $\pm 3\%$  as verified by a comparison of calculations using the Miner and Lewis<sup>10</sup> code. All the comparisons were made for an angle of attack of about 40 degrees.

To determine the consistency from flight to flight the bottom centerline heat flux measurements for STS-2, 3, and 5 are compared at three different times in the flights as shown in Figures 1, 2, and 3, respectively. The corresponding free-stream conditions are given in Table 2. It is seen that the flight-to-flight repeatability is about 15-30% and the standard deviation about the mean at each X/L

\* The author is grateful to S. D. Williams of Lockheed Engineering and Management Services, Co. for calculating the heat flux for this determination.

is about  $\pm 10\%$ . The STS-2 heat fluxes are consistently lower than the other two flights at almost all locations. The reason for this is not understood, but it may be related to a change in catalycity resulting from contamination of the surface or to a change in emittance. The heating rate correction for these cases is no larger than 5% as seen in Table 2. The measurement at  $X/L = 0.695$  seems anomalously low and therefore, it may be a bad measurement. The rather large discrepancy in the measurement for STS-2 compared with the other two flights at  $X/L = 0.14$  also is not understood.

#### SHUTTLE CENTERLINE PRESSURES

Pressure measurements during the time of high heating on the orbiter were obtained only during STS-3 and 5. These measurements normalized by  $\rho_\infty V_\infty^2$  are presented in figure 4 along with values calculated by three methods. It is seen that the flight-to-flight repeatability is very good at almost all locations. The pressure decreases very rapidly in the forward 10% of the vehicle then remains almost constant from  $X/L$  of 0.1 to 0.4, rising slightly at  $X/L = 0.8$ . The 3-D flowfield calculations of Rakich and Lanfranco<sup>2</sup> and Goodrich et al.<sup>11</sup> agree with the measurements within about 5% except in the vicinity of  $X/L = 0.1$  where the calculations are about 23% higher than the measurements. Likewise, the calculations using the Miner and Lewis<sup>10</sup> code agree within about 5% except at  $X/L = 0.1$ , where the agreement is within about 9%. The large discrepancy at  $X/L = 0.1$  may result from an experimental error due to a negative bias of unknown amount<sup>18</sup>. The instrumentation and signal processing of the pressure measurements only result in positive readings. The existence of a negative bias was indicated by a measurement that did not exceed zero until a time later than expected for the flight condition. See reference 18. If the error associated with the negative bias is small, then the calculations appear to be in error at  $X/L = 0.1$ . Although a direct comparison of the geometries has not been made, it is possible that the geometry descriptions in the flowfield codes do not adequately describe the vehicle as actually built; otherwise these codes do not adequately handle the rapid expansion around the nose, overpredicting the pressure (and heat flux) near  $X/L = 0.1$ .

#### HEAT FLUX COMPARISONS

In the following comparisons the author has used the results of others and in some cases has used the method of others to make present calculations. In these cases the author is responsible for any error or misapplication of the method, not the developers of the methods.

##### Equilibrium and Nonequilibrium - Two Layer Methods

It has been shown in the past that the heat flux predicted by equilibrium calculations and by reacting calculations with a fully catalytic wall are approximately equal. To verify this for the two boundary layer methods considered here comparisons were made between equilibrium results of Goodrich et al.<sup>11</sup> and the results obtained using the Rakich and Lanfranco<sup>2</sup> method. The freestream conditions are given in Table 3. In figure 5 the Goodrich equilibrium prediction is compared with two nonequilibrium boundary layer cases with fully catalytic walls. (Fully

catalytic here means  $\gamma_0 = \gamma_N = 1$ , vis-a-vis  $k_w = \infty$  or  $C_{O_w} = C_{N_w} = 0$ .) The edge conditions in the latter two cases are Goodrich equilibrium and Rakich and Lanfranco nonequilibrium. Given the same edge conditions it is seen that the equilibrium boundary layer calculation is about 15% lower than the all-nonequilibrium calculation over the entire length of the vehicle. Evidently, the transport of chemical energy by diffusion is more efficient in this case than via conversion of chemical energy to thermal energy which is then transported to the wall via conduction. The opposite result was obtained by Shinn et al.<sup>7</sup> who found the equilibrium viscous shock layer resulted in higher heating than the equilibrium catalytic wall nonequilibrium case.

The comparison of the reacting boundary layer with equilibrium edge conditions versus reacting edge conditions indicates that on the nose there is very little difference between the two cases, whereas on the midfuselage the nonequilibrium edge conditions results in about 15% lower heating. The nonequilibrium edge case with a fully catalytic wall is very close to the all equilibrium calculation aft of  $X/L = 0.2$ . The latter agreement does not stem from the flow approaching equilibrium downstream because the equilibrium nitrogen atom concentration both at the edge and in boundary layer is greater than the nonequilibrium concentration by a factor of about 1.3 in this case. Moreover, it was shown in reference 1 that the boundary layer is virtually frozen.

A comparison of the axisymmetric reacting viscous shock layer method of Miner and Lewis<sup>10</sup> and the reacting two-layer approach of Rakich and Lanfranco<sup>2</sup> is made in figure 6 where the nonequilibrium boundary layer result for a fully catalytic wall lies above the viscous shock layer results by about 20% on the nose. Agreement improves to within about 11% at  $X/L = 0.55$ . The effect of edge conditions is about 10% or less everywhere for a fully catalytic wall. The results for a noncatalytic wall are given in figure 7 where it is seen that the boundary layer heat flux is about 30% greater than the viscous shock layer heating on the nose, but improves to about 10% at  $X/L = 0.55$ . Agreement of the reacting viscous shock layer results and the reacting boundary layer with equilibrium edge conditions is within about 10% everywhere along the body. The equilibrium edge condition results fall below the nonequilibrium results on the nose, but they are very close farther aft.

Attention is now turned to a comparison of the axisymmetric viscous shock layer method of Moss<sup>9</sup> as applied by Shinn et al.<sup>7</sup>, and the two-layer method of Rakich and Lanfranco<sup>2</sup> applied here for a lower velocity and altitude situation. It is seen in figure 8a that the axisymmetric nonequilibrium viscous shock-layer with equilibrium catalytic wall (ECW) and the equilibrium viscous shock layer agree quite well (within about 5%). They also agree quite well with the Goodrich<sup>11</sup> equilibrium two-layer result. It is seen that the fully catalytic nonequilibrium two-layer results are greater by about 10-20% which is the same as noted for case 1. Agreement in figure 8b for the noncatalytic case is worse than the two-layer results, being about 20-40% higher than the axisymmetric viscous shock layer results of Shinn et al.<sup>7</sup> and present results using the Miner and Lewis<sup>10</sup> code. The latter results seem to indicate that heat transfer by atom diffusion is more important in the viscous shock layer. This is consistent with the somewhat higher degree of dissociation, especially the nitrogen, associated with the viscous shock layer calculation. The reason for the differences in atom fraction in the two methods is not understood since the reaction rates used in both methods were essentially the same.

The recent 3-D nonequilibrium viscous shock layer results with a noncatalytic wall are also given in figure 8b. The heat flux at  $X/L = 0.1$  is closer to the axisymmetric VSL results, but does not decrease as rapidly downstream. In fact, the 3-D results are higher than the two-layer results aft of  $X/L = 0.2$ . The chemical reaction model<sup>19</sup> in all the methods is virtually the same, (except ions are neglected in the Rakich and Lanfranco method). Therefore, the differences seen are most likely due to differences in the computational method or the geometry.

#### Comparison of Measured and Calculated Heat Flux

Attention is now turned toward a comparison of the calculated heat flux and the measured values along the lower surface centerline. The comparison is at two times in each of two flights. The particular times were selected to match the velocity and density as closely as practicable to the conditions used in the boundary layer predictions for cases 460 and 650 in Table 3. It was not possible to simultaneously match both velocity and density. The resulting heat fluxes were adjusted for the mismatch by the factor  $f$  of equation (2). As mentioned earlier the measured heat fluxes were inferred from the measured temperatures using equation (1) where  $\epsilon = 0.85$ .

Several choices of catalytic recombination coefficients were used as wall boundary conditions for the two layer and the axisymmetric shock layer calculations. The energy transfer catalytic recombination coefficients for nitrogen and oxygen recombination on the RCG tile coating are presented in figures 9 and 10, respectively. The coefficients presented are those found in references 6, 7, and 12. In those cases where a catalytic speed  $k_w$  was given the recombination coefficient is plotted as a dashed line, the length of which indicates the temperature range over which  $k_w$  was used, where

$$q = k_w \sqrt{2 \tau_m / kT}$$

It is seen in figure 9 that the inferred values of  $k_{wN}$  of reference 4 are 0.1 to 0.2 times the values of reference 6. This lack of agreement is not surprising since  $k_{wN}$  was assumed to be 0.3 times  $k_{wO}$  in reference 4. The values of  $k_{wO}$  (see figure 10) of references 4 and 6 agree within experimental accuracy at the higher temperature range. At lower temperatures  $k_{wO} = 80$  cm/sec is about a factor of 1.5 to 3 higher than the extrapolation of reference 6, depending on temperature.

Extrapolating to such a low temperature could be inaccurate, but the extrapolation is generally consistent with other recombination measurements (see figure 6 of reference 4). Since the temperatures measured on the Shuttle fell mostly in the lower temperature range 900-1100 K, the predictions of heat flux using the  $k_{wO} = 80$  cm/sec would result in higher heating except on the nose or earlier in time where the nitrogen carries a larger part of the dissociation energy.

A comparison is made in figures 11-14 between the measurements and several calculations for STS-2 and 3 at two times in the trajectories. The measurements are near the bottom centerline of the vehicle except for a few points that are about 1.3 m off the centerline. This comparison between the calculations and the measurements is typical for all times and both flights. In the higher altitude cases (figures 11 and 13) the viscous shock layer methods with the temperature dependent values<sup>6</sup> of  $k_{wO}$  and  $k_{wN}$  yield better agreement for  $X/L < 0.3$ . The two layer method with  $k_{wO} = 80$  cm/sec also agrees with the measurements at  $X/L > 0.3$ . At the lower



altitude (figures 12 and 14) the two-layer methods yield better agreement for  $X/L > 0.2$ .

In the higher altitude cases (figures 11 and 13), the nonequilibrium axisymmetric viscous shock layer methods with the temperature dependent  $Y_O$  and  $Y_N$ , yield good agreement at  $X/L < 0.3$  and the nonequilibrium two layer method with  $k_{wO} = 80$  cm/sec and  $k_{wN} = 24$  cm/sec yields good agreement for  $X/L < 0.5$ . For the lower altitude case this two-layer approach yields better agreement for  $X/L > 0.2$  than the axisymmetric viscous shock layer methods. The nonequilibrium two-layer method using temperature dependent  $Y_O$  and  $Y_N$  results are about 30% higher than the measurements on the nose area for all cases presented here, but the agreement improves toward the mid-vehicle and at lower altitude. It is apparent that the two-layer approach predicts higher heat fluxes for given wall boundary conditions than the viscous shock layer approaches. This may be due in part to the VSL having a slightly higher level of dissociation as well as to differences in the flowfield dynamics.

In comparing the 3-D nonequilibrium calculations of Kim, Swaminathan and Lewis<sup>3</sup> with other noncatalytic predictions, one sees that the heat flux does not decrease as rapidly down the vehicle as do the axisymmetric viscous shock layer calculations and the two layer calculations. This indicates a possible influence of geometry and cross flow that is more adequately accounted for in the 3-D viscous shock layer model. In figures 11 and 12 the 3-D viscous shock layer results of reference 8 tend toward better agreement with the measurements than the other calculations aft of  $X/L = 0.6$ . This 3-D approach should be further investigated with appropriate finite rate recombination coefficients.

The increase in measured heat flux above the calculations on aft half of the vehicle and especially for the later flight may also have other explanations. The increase could be due to increasing recombination rates, but that would be inconsistent with the measurements on the forward part of the vehicle unless the aft is contaminated with a catalytic material. This is possible because the adhesive used to bond tiles to the structure contains various metal oxides, particularly iron oxide which is known to be highly catalytic.

The two-layer methods have been used to calibrate faster and more flexible codes to provide heat fluxes and other properties over a wider range of conditions than for which the two-layer methods were applied. The nonequilibrium results of Rakich and Lanfranco<sup>2</sup> have been used by Rakich, Stewart and Lanfranco<sup>4</sup> and by Scott and Derry<sup>5</sup>. One of the weaknesses of these applications is the inability to properly account for variations in the flowfield chemical composition as parameters such as the angle of attack, freestream density and velocity differ from the few cases available from the 3-D Euler solutions. The axisymmetric shock layer codes have the advantage that they are more flexible in running cases because of their fast computation time. Gupta et al.<sup>13</sup> investigated the influence of small variations in angle of attack on the nonequilibrium heating and found the influence on heat flux to be small. A larger percentage variation was observed for lower velocities. This may be due to greater temperature sensitivity of the level of oxygen dissociation at lower temperatures rising in the lower altitude case. Small changes in the component of velocity normal to the shock wave associated with the change in angle of attack result in temperature changes in a range in which the oxygen dissociation is very sensitive. However, since the general sensitivity of absolute heat flux to angle of attack is small, the approximations made in references 4 and 17 should not

be very significant in this regard.

The disadvantage of the axisymmetric viscous shock layer methods is that they are only capable of handling bodies of revolution and they rely on angle of attack simulation via changing the body profile. Cross flow or transverse body curvature is therefore quite limited. Fortunately, for the present work this has not been a strong limitation but it may explain why there is disagreement with measurements on the aft of the vehicle.

The 3-D viscous shock layer approach does away with those approximations, but suffers from the requirement of a shock shape as input (as do the axisymmetric viscous shock layer solutions). The 3-D version has only recently been developed and will require further work to compare with measurements before its adequacy will be known.

The 3-D inviscid solution method coupled with boundary layer solutions requires very much computer time to obtain the inviscid flowfield and requires assumptions about how far into the inviscid flow from the body to go to obtain boundary layer edge conditions. Choosing the boundary layer edge too far into the lower entropy flowfield will result in heating predictions that are too high. This may be the reason that the two-layer methods predicted higher results than the axisymmetric viscous shock layer method for the noncatalytic case at  $X/L > 0.02$  and for the fully catalytic case at  $0.02 < X/L < 0.2$ . The noncatalytic case is more sensitive to the dissociation level which is higher in the flow from the normal shock region.

Inferring catalytic recombination rates from the flight measurements is made difficult for several reasons. First, the flowfield is composed of oxygen and nitrogen atoms in varying amounts according to the vehicle trajectory and location on the vehicle. If one chooses a lower velocity condition where very little nitrogen is dissociated then it may be possible to infer  $k_{wO}$ . However, we have seen a flight-to-flight measurement uncertainty of at least 15% and prediction-to-prediction variation of the same magnitude. Heating uncertainties of this magnitude result in  $k_w$  uncertainties on the order of a factor of 5 (see reference 13). Therefore, such a procedure should be used with great caution. This illustrates the need for careful ground experiments or great fidelity in the flight heat flux calculations to obtain accurate recombination coefficients. The ground measurements of Scott<sup>6,14</sup>, as with any ground measurements, require either precise heat flux calculations and/or a reliable reference surface with which to compare the heating. Even then accurate results are difficult. Fortunately only moderately accurate recombination coefficients are required to calculate reasonably accurate heating rates.

To ascertain the nitrogen recombination coefficients from flight measurements is almost impossible without knowledge of the coefficients for oxygen because the oxygen atom is always an important species in the flow whenever there is any nitrogen dissociated. If the flowfield and  $k_{wO}$  were known accurately as a function of  $T_w$  then it might be possible to infer  $k_{wN}$ .

#### Heating to Highly Catalytic Tiles

Attention is now turned to the results of the Ames Research Center's catalytic surface effects orbiter experiment<sup>3,4</sup>. Not only did this very significant

experiment demonstrate the noncatalytic nature of the RCG coated tiles, but it also may give some clues as to the variation of dissociation in the boundary layer and the wall recombination rates. On STS-2 two tiles were painted with a highly catalytic material, iron-cobalt-chromia spinel (C742), developed by Stewart et al.<sup>3</sup> at the Ames Research Center. The predicted and measured heat fluxes in the vicinity of the two C752-coated tiles on the bottom centerline of the orbiter during STS-2 reentry are given in figures 15 and 16. The measurements were obtained at 475 sec after 122 km altitude was reached. At the forward location near the nose, the two-layer calculation using the method and recombination rates of Rakich et al.<sup>4</sup> yields the best agreement with the measurements. This should be the case because the recombination coefficients were inferred from the measurements at this location and approximate entry time. Also shown is the same calculation but using recombination coefficients obtained from arc jet measurements<sup>6,14</sup>. As seen in figure 15, (the forward location), the increase in heat flux on the C742-coated tile is larger for the Rakich recombination rates than for the recombination rates of references 6 and 14, even though the latter rates for C742 are larger. The reason for this behavior is that, due to the higher RCG recombination rates of reference 6, the boundary layer is depleted of atomic nitrogen and oxygen so that when the flow reaches the C742-coated tile there is not as much chemical energy available for transfer to the highly catalytic tile. A similar behavior is seen at  $X/L = 0.4$  in figure 16. Since the recombination rates of references 6 and 14 increase with temperature, the upstream edge of the C742-coated tile sees a high heat flux that decreases rapidly because of depletion of atoms in the boundary layer and this leads to further reduction in recombination rate along the tile as the temperature decreases.

The agreement between the axisymmetric viscous shock layer method and the boundary layer method is not very good on the C742-coated tiles. The heat flux drops much more rapidly, possibly because of more rapid depletion of atoms in the boundary layer, than the boundary layer method predicts. There also seems to be some sensitivity of the heat flux distribution along the tile to the streamwise nodal spacing used in the calculation.

#### CONCLUDING REMARKS

This paper has attempted to evaluate the current state-of-the-art nonequilibrium flow tools applied to the Space Shuttle. From this discussion the importance of nonequilibrium phenomena to the Space Shuttle reentry heating has been assessed. Since the inception of the design of the Space Shuttle over fourteen years ago there have been developments in the heat flux prediction methodologies. Initially nonequilibrium and surface catalysis effects were ignored. This led to a design that exceeded the requirements in many areas, but also resulted in an added margin of safety in other areas that proved beneficial.

It was found that the heat fluxes measured on the windward centerline of the orbiter tended to increase from flight to flight. Roughly, a 20% change was noted from STS-2 to 5 at most of the thermocouple locations, indicating changes in surface properties such as emittance or catalycity.

The nonequilibrium heat flux methods that have been developed and the catalycity measurements obtained over the past decade have improved the prediction

capability from a 20 to 100% overprediction for an assumed fully catalytic surface material to an accuracy of about 10 to 30% for nearly noncatalytic materials, e.g., the RCG coating on HRSI. These methods are the two-layer inviscid 3-D reacting flowfield coupled with the reacting boundary layer, and the reacting viscous shock layer solutions. The application of these methods may result in less reliance on wind tunnel measurements which cannot simulate the high enthalpy reacting flows associated with orbital reentry. Indeed the calculations are necessary for such a simulation.

As the comparisons of the predictions with the measurements from the Space Shuttle flight tests have shown, we are now in a position of refining the prediction techniques and determining those phenomena that will be of significance for the design of future reentry vehicles such as an aerobraking orbital transfer vehicle (AOTV).

Although nonequilibrium calculation techniques using finite rate catalytic wall boundary conditions has significantly improved the prediction capability, none of the methods yields good agreement uniformly for all locations and freestream conditions. This points to the need for further refinement in these methods. The 3-D viscous approaches in particular should be pursued since the trends of the heating profiles tend to be better than for the other methods.

Nitrogen recombination is seen to be a very important phenomenon, particularly on the nose and elsewhere at the higher velocities. This means that the accuracy of the nitrogen recombination coefficients is important to the heat flux predictions in those areas. Since the AOTV enters the atmosphere at higher speeds and remains at higher altitudes where nonequilibrium flow dominates, the nitrogen gas and surface reactions will be especially important.

#### REFERENCES

1. Scott, C. D., "Space Shuttle Laminar Heating with Finite-Rate Catalytic Recombination," Thermophysics of Atmospheric Entry, Progress in Astronautics and Aeronautics, Vol. 77, edited by T. E. Horton, AIAA, New York, 1982, pp. 273-289.
2. Rakich, J. V. and Lanfranco, M. J., "Numerical Computation of Space Shuttle Laminar Heating and Surface Streamlines," Journal of Spacecraft and Rockets, Vol. 14, May 1977, pp. 265-272.
3. Stewart, D. A., Rakich, J. V. and Lanfranco, M. J., "Catalytic Surface Effects Experiment on the Space Shuttle," in Thermophysics of Atmospheric Entry, Vol. 82 of Progress in Astronautics and Aeronautics, 1982, T. E. Horton, Editor, pp. 248-272.
4. Rakich, J. V., Stewart, D. A. and Lanfranco, M. J., "Results of a Flight Environment on the Catalytic Efficiency of the Space Shuttle Heat Shield," AIAA Paper 82-0944, AIAA/ASME 3rd Joint Thermophysics, Fluids, Plasma and Heat Transfer Conference, June 7-11, 1982, St. Louis, MO.
5. Scott, C. D. and Derry, S. M., "Catalytic Recombination and the Space Shuttle Heating," AIAA Paper 82-0841, AIAA/ASME 3rd Joint Thermophysics, Fluids, Plasma and Heat Transfer Conference, June 7-11, 1982, St. Louis, MO.
6. Scott, C. D., "Catalytic Recombination of Oxygen and Nitrogen in High Temperature Reusable Surface Insulation," in Aerothermodynamics and Planetary Entry, edited by A. L. Crosbie, Vol. 77 of Progress in Astronautics and Aeronautics, 1981, pp. 192-212.
7. Shinn, J. L., Moss, J. N. and Simmonds, A. L., "Viscous-Shock-Layer Heating Analysis for the Shuttle Windward Plane with Surface Finite Catalytic Recombination Rates," AIAA Paper 82-0842, AIAA/ASME 3rd Joint Thermophysics Fluids, Plasma and Heat Transfer Conference, June 7-11, 1982, St. Louis, MO.
8. Kim, M. D., Swaminathan, S. and Lewis, C. H., "Three-Dimensional Nonequilibrium Viscous Shock Layer Flows Over the Space Shuttle Orbiter," AIAA Paper 83-0487, AIAA 21st Aerospace Sciences Meeting, January 10-18, 1983, Reno, NV.
9. Moss, J. N., "Reacting Viscous Shock-Layer Solutions with Multicomponent Diffusion and Mass Injection," NASA TR R-411, June 1974.
10. Miner, E. W. and Lewis, C. H., "Hypersonic Ionizing Air Viscous Shock-Layer Flows Over Nonanalytical Blunt Bodies," NASA CR-2550, May 1975.
11. Goodrich, W. D., Li, C. P., Houston, C. K., Chin, P. B. and Olmedo, L., "Numerical Computations of Orbiter Flowfields and Laminar Heating Rates," Journal of Spacecraft and Rockets, Vol. 14, May 1977, pp. 257-264.

12. Zoby, E. V., "Analysis of STS-2 Experimental Heating Rates and Transition Data," AIAA/ASME 3rd Joint Thermophysics Fluids, Plasma and Heat Transfer Conference, June 7-11, 1982, St. Louis, MO.
13. Gupta, R. N., Moss, J. H., Simmonds, A. L., Shinn, J. L. and Zoby, E. V., "Space Shuttle Heating Analysis with Variation in Angle-of-Attack and Surface Condition," AIAA Paper 83-0486, AIAA 21st Aerospace Sciences Meeting, January 10-13, 1983, Reno, NV.
14. Scott, C. D., "Catalytic Recombination of Nitrogen and Oxygen on Iron-Cobalt-Chromia Spinel," AIAA Paper 83-0585, January 1983, Reno, NV.
15. Bartlett, E. P. and Kendall, R. M., "An Analysis of the Coupled Chemically Reacting Boundary Layer and Charring Ablator, Pt. III: Nonsimilar Solution of the Multicomponent Laminar Boundary Layer by an Integral Matrix Method," NASA CR-1062, June 1968.
16. Tong, N., Buckingham, A. C. and Morse, H. L., "Nonequilibrium Chemistry Boundary Layer Integral Matrix Procedure," NASA CR-134039, July 1973.
17. Williams, S. D. and Curry, D. M., "An Analytical and Experimental Study for Surface Heat Flux Determination," Journal of Spacecraft and Rockets, Vol. 14, No. 10, October 1977, pp. 632-637.
18. Bradley P. F. Siemers, P. M., III and Weilmuenster, K. J., "An Evaluation of Space Shuttle Orbiter Forward Fuselage Surface Pressures: Comparison with Wind Tunnel and Theoretical Predictions," AIAA Paper 83-0119, AIAA 21st Aerospace Sciences Meeting, January 10-13, 1983, Reno, NV.
19. Blottner, F. G., "Nonequilibrium Laminar Boundary-Layer Flow of Ionized Air," General Electric Report R64SD56, November 1964.

TABLE 1 - METHODS AND APPLICATIONS PRESENTED IN PLOTS

Application No.	Method	Application	Wall Boundary Condition	Flow Field	Boundary Layer Edge Condition	Chemistry of B.L.
1	Moss <sup>9</sup>	Shinn, et al <sup>7</sup>	Scott <sup>6</sup>	VSL+ Noneq.	N/A	N/A
2	"	"	ECW*	"	"	"
3	"	"	Noncata.	"	"	"
4	"	"	Equilib.	VSL Equilib.	"	"
5	Miner & Lewis <sup>10</sup>	Present	Scott <sup>6</sup>	VSL Reacting	"	"
6	"	"	Fully Cata.	"	"	"
7	"	"	Noncata.	"	"	"
8	Goodrich, et al <sup>11</sup>	Goodrich, et al <sup>11</sup>	Equilib.	3-D Inviscid Equilib.	Equilib.	Equilib.
9	Rakich, et al <sup>2</sup>	Present	Fully Cata.	3-D Inviscid Noneq.	Noneq.	Noneq.
10	"	"	Scott <sup>6</sup>	"	"	"
11	"	"	Noncata.	"	"	"
12	Goodrich, et al <sup>11</sup>	"	Fully cata.	"	Equilib.	"
13	"	"	Scott <sup>6</sup>	"	"	"
14	"	"	Noncata.	"	"	"
15	Rakich, et al <sup>2</sup>	"	Rakich, et al <sup>4</sup>	"	Noneq.	"
16	Kim, et al <sup>14</sup>	Kim, et al	Noncata.	3-D VSL Noneq.	N/A	N/A

\* ECW = Equilibrium Catalytic Wall  
 + VSL = Viscous Shock-Layer

ORIGINAL PAGE 13  
OF POOR QUALITY

TABLE 2 - FREESTREAM CONDITIONS<sup>c</sup> FOR CORRESPONDING  
HEAT FLUX MEASUREMENTS

Flight	time <sup>b</sup> sec	V <sub>∞</sub> km/sec	ρ <sub>∞</sub> kg/m <sup>3</sup>	α deg	f <sup>a</sup>	Z km	h <sub>∞</sub> MJ/kg	ρ <sub>∞</sub> V <sub>∞</sub> <sup>2</sup> kPa
STS-2	475	7.16	.412-4	40.37	1.000	74.7	25.6	2.11
	700	5.57	.807-4	39.99	1.000	70.2	21.6	3.49
	10 <sup>6</sup>	4.56	.402-3	40.56	1.000	57.2	12.4	8.35
STS-3	400	7.29	.394-4	40.02	1.033	75.1	25.6	2.09
	700	5.29	.113-3	39.58	1.037	68.2	19.8	4.46
	960	4.58	.417-3	40.72	1.032	57.6	12.5	8.75
STS-5	400	7.17	.408-4	40.05	.998	74.9	25.7	2.09
	700	6.19	.164-3	40.71	.950	61.9	19.2	3.99
	950	4.56	.441-3	39.19	1.076	54.0	12.4	9.16

- a  $f = (\rho/\rho_{ref})^{1/2} (V/V_{ref})^3$  Factor used to adjust heat flux relative to STS-2 condition, based on stagnation point theory.
- b Time from entry interface (Z = 122 km)
- c Best Estimated Trajectory

TABLE 3 - FREESTREAM CONDITIONS FOR CALCULATIONS

Case No.	1	1	2	460 <sup>a</sup>	650 <sup>a</sup>
Method	BL	VSL	BL	VSL	VSL
Velocity, km/s	7.62	7.62	6.514	7.20	6.73
Attitude, km	75.0	75.0	68.9	75.0 <sup>c</sup>	71.3
Angle-of-Attack, deg	41.4	41.4	40.2	40.0	39.4
Density, kg/m <sup>3</sup>	3.795-5	3.974-5	9.28-5	3.81-5	6.83-5
Total Enthalpy, MJ/kg	29.0	29.0	21.3	25.9	22.6
Temperature, K	197.	197.	221.	198.	205.
Stagnation Point Pressure, kPa	2.20	2.31	4.10	1.98	3.09
Noise Radius, m	0.814	1.342	0.814	1.276	1.253
Hyperboloid angle <sup>b</sup> , deg	-	47.2	-	40.75	40.20
Lewis No. in Shock Layer					
Present Calculations	-	1.0	-	1.0	1.0
Reference 11	-	1.4	-	1.4	1.4
Reference 16	-	1.4	-	1.4	1.4

- a These freestream conditions are the same as the one in reference 7 for STS-2 times corresponding to the case number and the same as cases 2 and 3 in reference 8.
- b Not applicable to 3-D VSL.



ORIGINAL PAGE IS  
OF POOR QUALITY

SHUTTLE CENTERLINE HEAT FLUX  
REFERENCE IS STS-2 VINP=7.16 km/S ALT=74.7 km

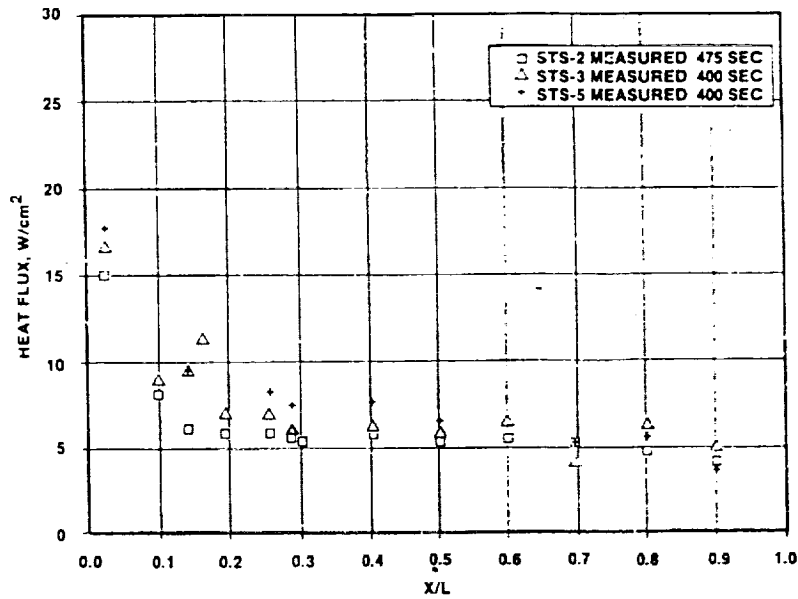


Figure 1.- Measured radiation equilibrium heat fluxes near windward centerline of orbiter. Altitude = 74.7 km.

SHUTTLE CENTERLINE HEAT FLUX  
REFERENCE IS STS-2 VINP=6.57 km/S ALT=70.2 km

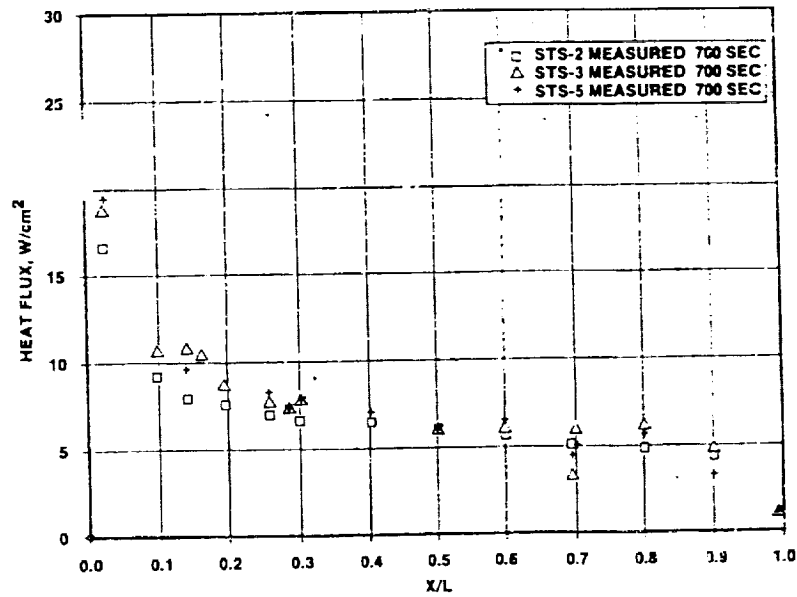


Figure 2.- Measured radiation equilibrium heat fluxes near windward centerline of orbiter. Altitude = 70.2 km.

SHUTTLE CENTERLINE HEAT FLUX  
 REFERENCE IS STS-2 VINF=4.56 km/S ALT=57.2 km

ORIGINAL PAGE IS  
 OF POOR QUALITY

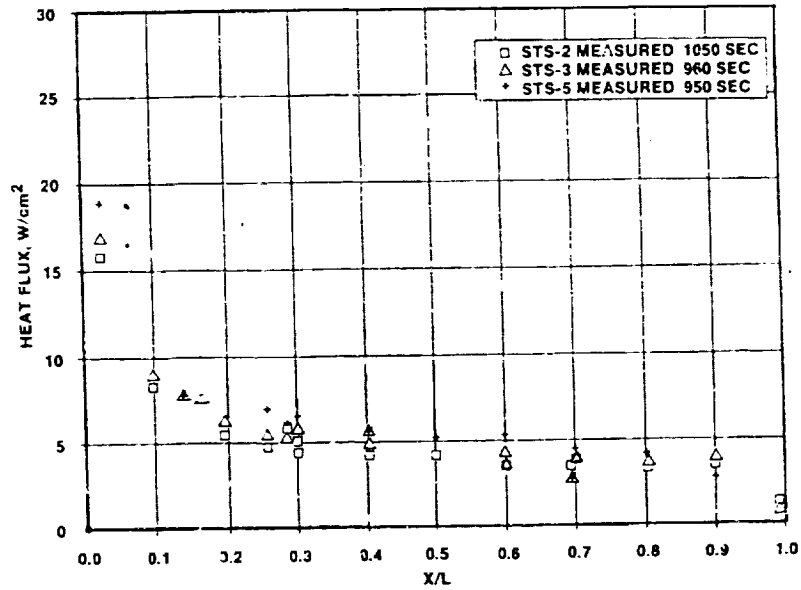


Figure 3.- Measured radiation equilibrium heat fluxes near windward centerline of orbiter. Altitude = 57.2 km.

SHUTTLE CENTERLINE PRESSURE  
 T=460 SEC VINF=7.2 km/S ALT=74.3 km

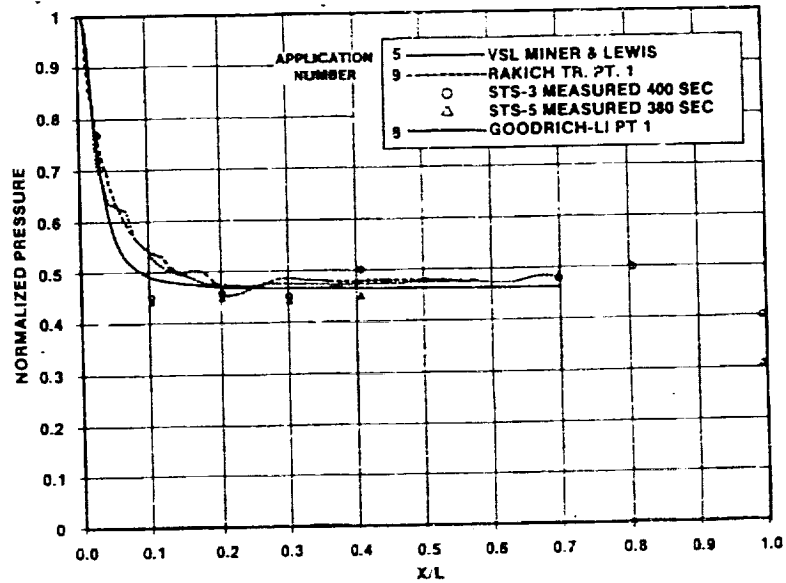


Figure 4.- Measured and calculated pressures on centerline of orbiter.

SHUTTLE CENTERLINE HEAT FLUX  
CASE 1 VIN<sub>F</sub>=7.62 km/SEC ALT=7438 km  
BOUNDARY LAYER CALCULATIONS

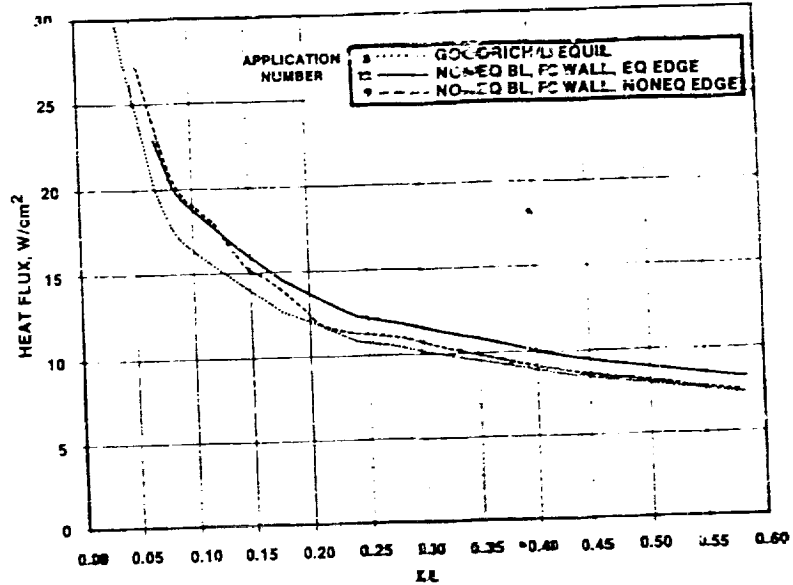


Figure 5.- Comparison of equilibrium and nonequilibrium boundary layer calculations with fully catalytic wall.

SHUTTLE CENTERLINE HEAT FLUX  
CASE 1 VIN<sub>F</sub>=7.62 km/SEC ALT=7438 km

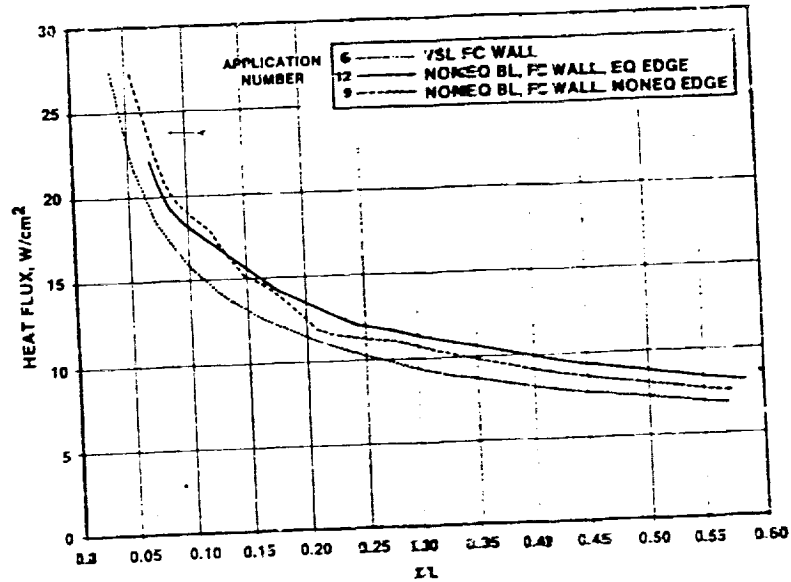


Figure 6.- Comparison of nonequilibrium axisymmetric viscous shock layer and two-layer calculations with fully catalytic wall.

ORIGINAL PAGE IS  
OF POOR QUALITY

SHUTTLE CENTER' NE HEAT FLUX  
CASE 1 VIN<sub>F</sub>=7.62 km/SEC ALT=74.38 km

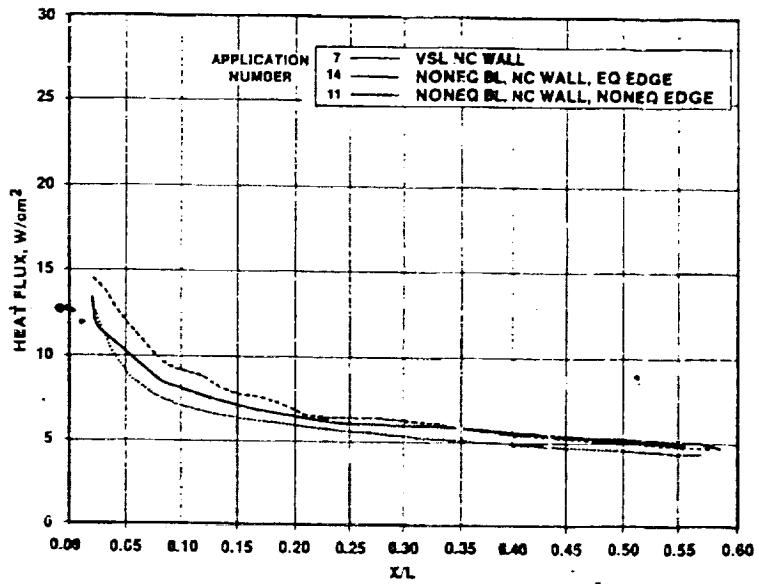
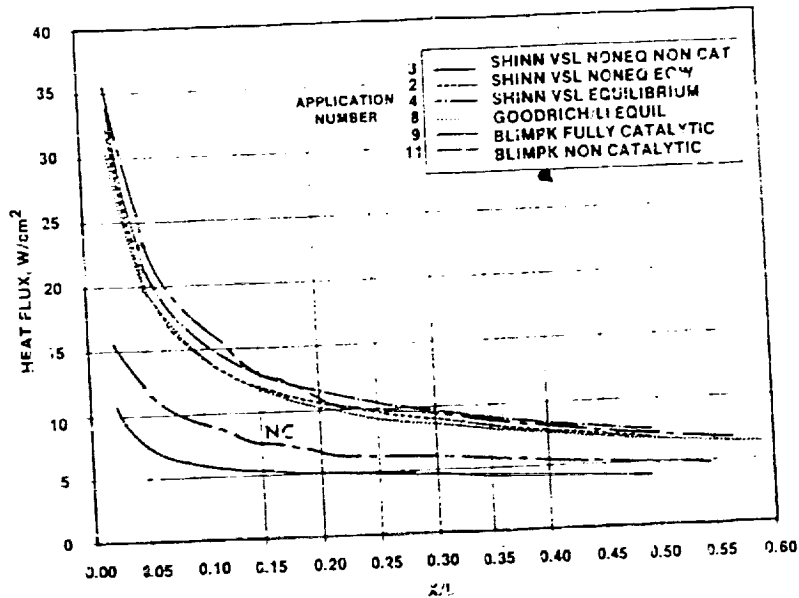


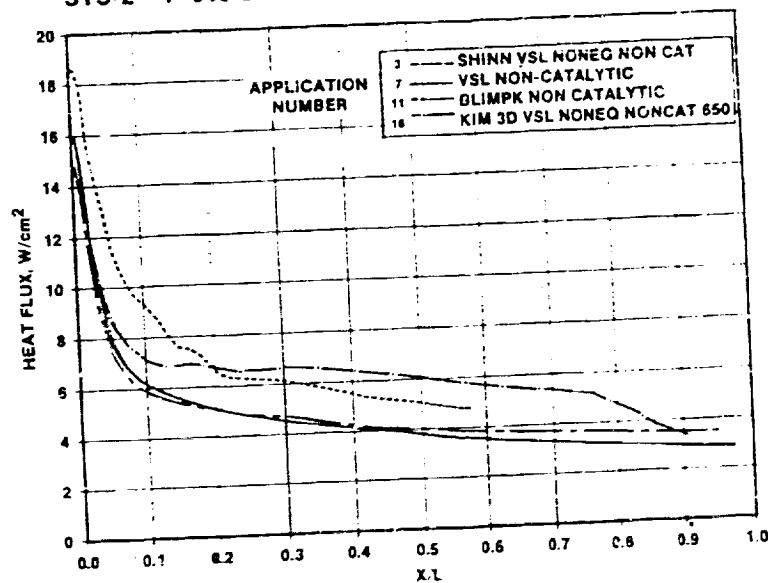
Figure 7.- Comparison of nonequilibrium axisymmetric viscous shock layer with two-layer calculations having nonequilibrium and equilibrium edge conditions for noncatalytic wall.

SHUTTLE CENTERLINE HEAT FLUX  
STS-2 T=650 SEC VINP=6.73 km/S ALT=71.29 km



(a) Comparison of axisymmetric viscous shock layer and two-layer calculations for STS-2 650-sec case.

SHUTTLE CENTERLINE HEAT FLUX  
STS-2 T=650 SEC VINP=6.73 km/S ALT=71.29 km



(b) Comparison of nonequilibrium axisymmetric and 3-D viscous shock layer and two-layer calculations with noncatalytic wall.

Figure 8.- Comparison of available prediction methods for Shuttle centerline heat flux.

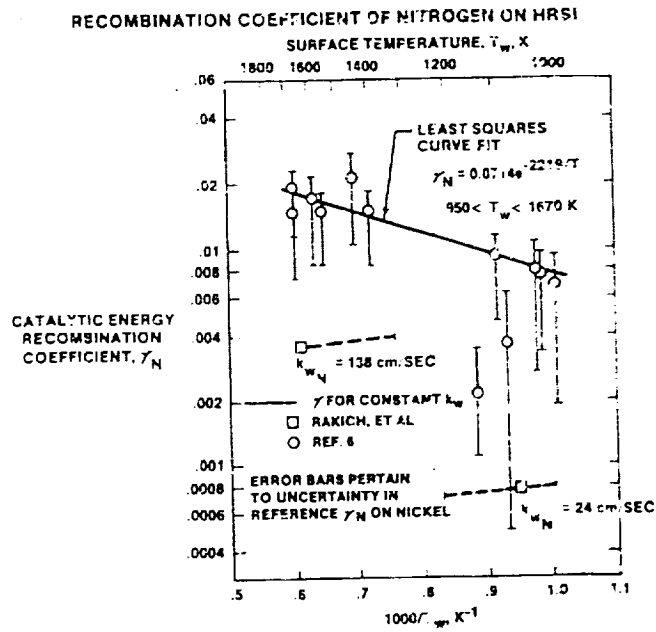


Figure 9.- Energy transfer catalytic recombination coefficient for nitrogen on RCG-coated HRSI.

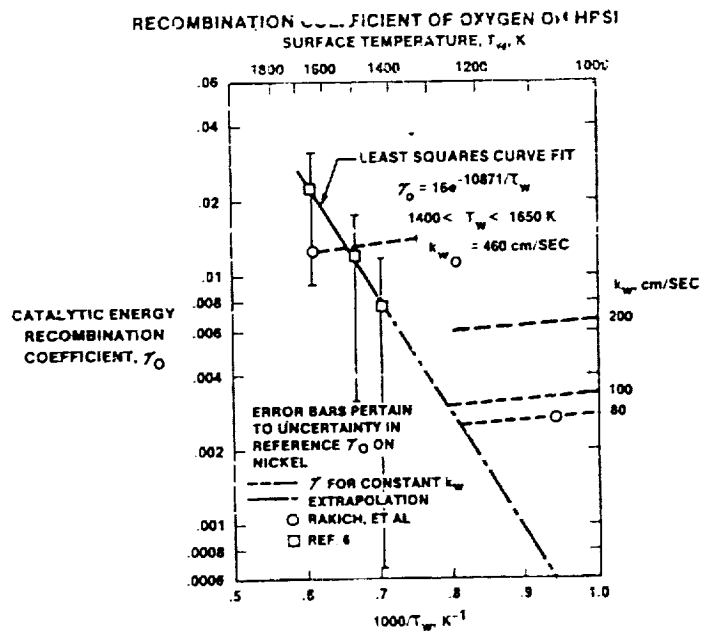


Figure 10.- Energy transfer catalytic recombination coefficient for oxygen on RCG-coated HRSI.

SHUTTLE CENTERLINE HEAT FLUX  
 STS-2 VINP=7.16 km/S ALT=74.7 km

ORIGINAL PRICE IS  
 OF POOR QUALITY

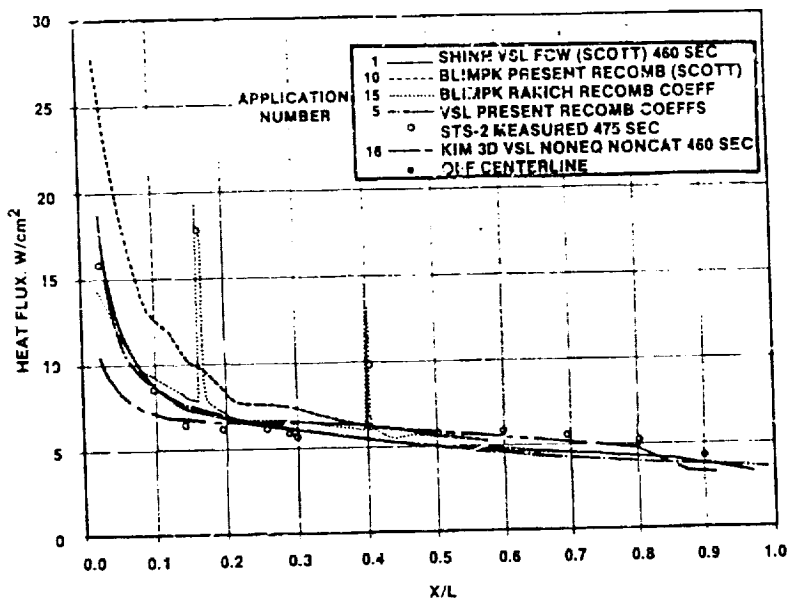


Figure 11.- Comparison of calculated and measured Shuttle heat fluxes for STS-2.  $t = 475$  sec; altitude = 74.7 km.

SHUTTLE CENTERLINE HEAT FLUX  
 STS-2 VINP=6.73 km/S ALT=71.29 km

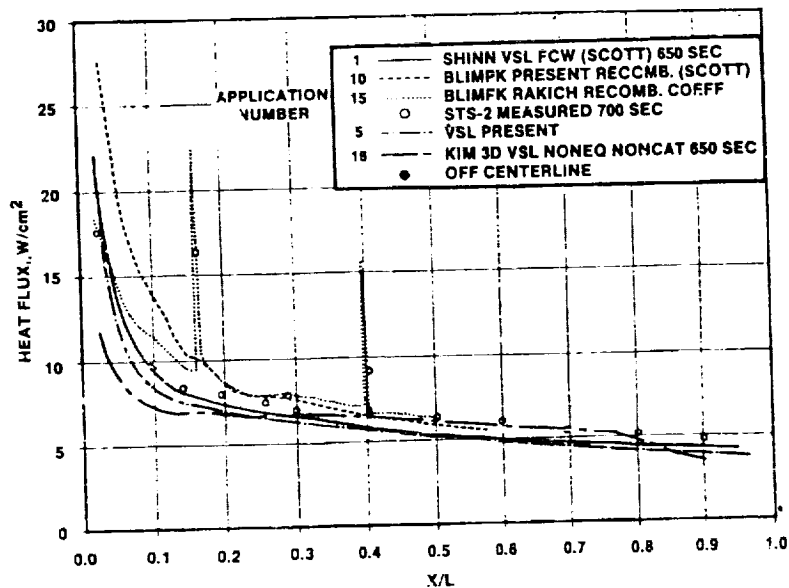


Figure 12.- Comparison of calculated and measured Shuttle heat fluxes for STS-2.  $t = 475$  sec; altitude - 71.29 km.

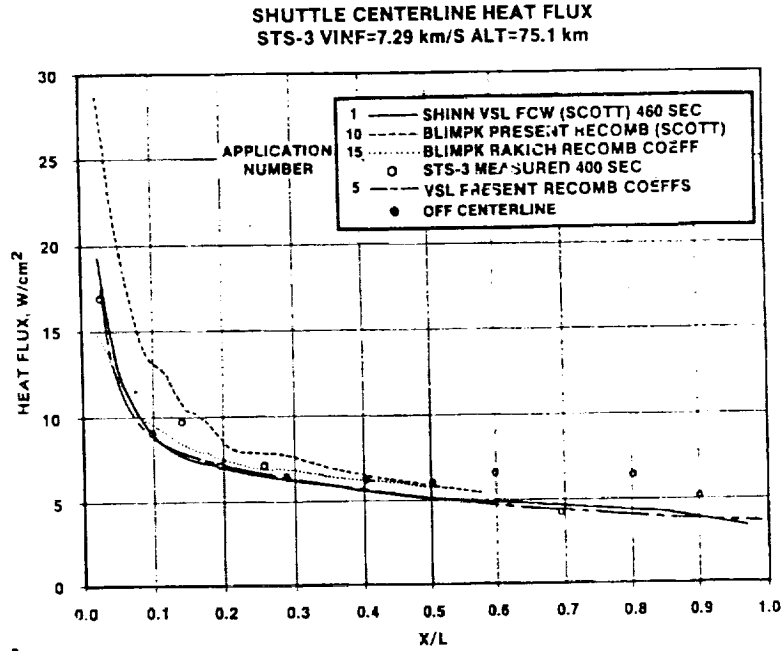


Figure 13.- Comparison of calculated and measured Shuttle heat fluxes for STS-3.  $t = 400$  sec.

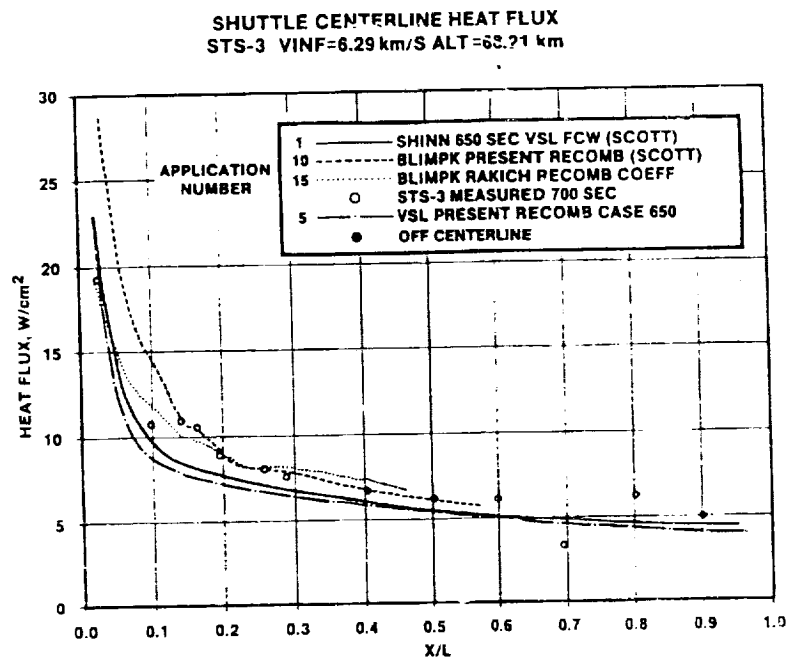


Figure 14.- Comparison of calculated and measured Shuttle heat fluxes for STS-3.  $t = 700$  sec.



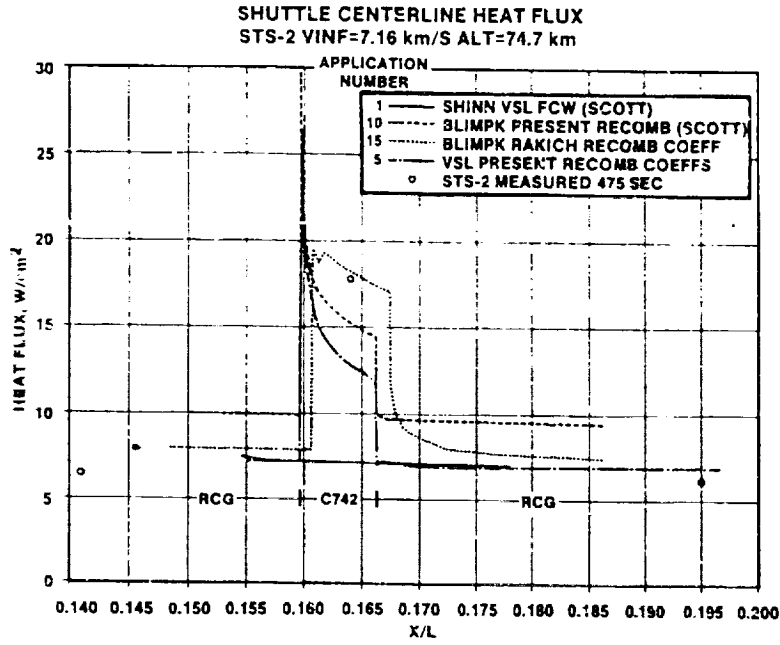


Figure 15.- Heat fluxes on C742-coated tile at X/L = 0.163 for STS-2. t = 650 sec.

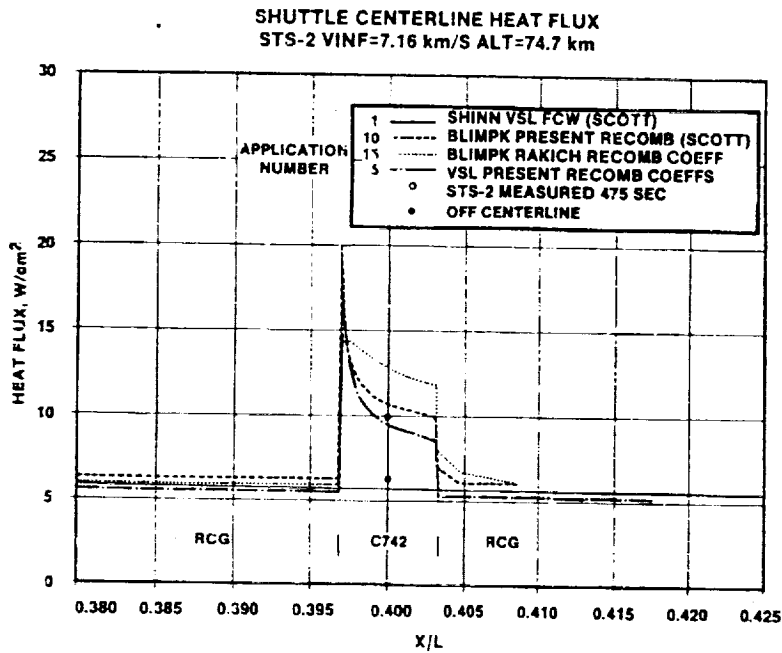


Figure 16.- Heat fluxes on C742-coated tile at X/L = 0.40 for STS-2. t = 650 sec.